Journal of the European Ceramic Society **12** (1993) 421–429

Reversible $\alpha \rightleftharpoons \beta$ Sialon Transformation in Heat-Treated Sialon Ceramics

H. Mandal, D. P. Thompson*

Materials Division, Department of Mechanical, Materials and Manufacturing Engineering, University of Newcastle upon Tyne, NE1 7RU, UK

&

T. Ekström

Arrhenius Laboratory, Department of Inorganic Chemistry, University of Stockholm, S-10691, Sweden

(Received 16 March 1993; revised version received 2 June 1993; accepted 15 June 1993)

Abstract

Typical β-sialon and mixed α–β-sialon starting compositions have been densified by pressureless sintering using either Ln_2O_3 or equimolar mixtures of $Ln_2O_3 + Y_2O_3$ where Ln = Sm, Dy, Yb. The resulting materials were heat treated at 1000–1500°C to devitrify the grain boundary glass into crystalline oxynitride phases. The effects of rare earth ionic size and heat-treatment temperature on the stability of devitrified phases, microstructure and mechanical properties have been studied. Microstructural characterisation of the α-sialon phase formed in these systems revealed that α is only stable at high temperatures and transforms to β-sialon plus grain boundary phases at lower temperatures; this provides an excellent mechanism for controlling the mechanical properties of the final material.

Typische β-Sialon und α–β Sialon Ausgangsmischungen wurden durch druckloses Sintern unter Verwendung von Ln_2O_3 oder einem equimolaren Gemisch aus $Ln_2O_3 + Y_2O_3$ verdichtet, wobei Ln = Sm, Dy, Yb bedeutet. Die sich daraus ergebenden Materialien wurden bei 1000–1500°C wärmebehandelt, um die Glasphase an den Korngrenzen in kristalline Oxyniridphase umzuwandeln. Der Einfluß der Größe seltenener Erdmetallionen und der Wärmebehandlungstemperatur auf die Stabilität der umgewandelten Glasphase, das Gefüge und die mechanischen Eigenschaften wurde untersucht. Die Gefügecharakterisierung der α-Sialonphase, die sich in diesem System bildet, ergab, daß α nur bei hohen Temperaturen stabil ist und sich bei niedrigen Temperaturen in β-Sialon und Korngrenzenphase umwandelt. Dieser Mechanismus bietet eine exzellente Möglichkeit, die mechanischen Eigenschaften des Endmaterials einzustellen.

Des mélanges initaux usuels de sialon β et de sialon mixte α–β ont été densifiés par frittage sous pression, en utilisant soit Ln_2O_3, soit des mélanges équimolaires $Ln_2O_3 + Y_2O_3$, où Ln = Sm, Dy, Yb. Les matériaux obtenus ont été soumis à un traitement thermique à 1000–1500°C afin que la phase amorphe présente aux joints de grains cristallise en phases oxynitrures. On a étudié l'effet du rayon ionique des terres rares employées et de la température de traitement sur la stabilité de ces phases, leur microstructure, leurs propriétés mécaniques. La caractérisation microstructurale du sialon α qui se forme dans ces systèmes montre que la phase α n'est stable qu'à haute température, et se transforme en un mélange de sialon β et de phase intergranulaire à basse température; ce mécanisme fournit un excellent moyen pour maîtriser les propriétés mécaniques du produit final.

1 Introduction

Sialon ceramics offer the advantage of easier densification by pressureless sintering compared with β-Si_3N_4 because of the lower eutectic temperature ($\approx$1300°C) in five-component M–Si–Al–O–N systems. The products nevertheless retain favourable mechanical, thermal and chemical properties up to these temperatures.[1]

* To whom correspondence should be addressed.

Journal of the European Ceramic Society 0955-2219/93/$6.00

The most important sialon phases are β, of general formula $Si_{6-z}Al_zO_zN_{8-z}$ $(0 \leq z \leq 4)$, and α, of general formula $M_x(Si,Al)_{12}(O,N)_{16}$ $(0 \leq x \leq 2)$, where M is Li, Mg, Ca, Y and Ln where Ln $\geq$ 60. Ekström and Ingelström[2] have shown that the mechanical properties of α–β-sialon composites can be optimised by adjusting the α:β-sialon ratio. The α-phase forms equiaxed microstructures of high hardness, whereas β-phase forms more elongated grains, giving microstructures which display high strength and increased fracture toughness ($K_{IC} \leq$ 9 MPa $m^{1/2}$).

The oxide densification additives used for sintering are generally insoluble in the β-sialon structure and even though most of them are α-sialon formers, some additive remains as a residual M–Si–Al–O–N intergranular glassy phase which degrades the mechanical and chemical properties of the material above the glass-softening temperature (900–1100°C).

Heat treatment is one of the accepted methods for eliminating (or minimising) the grain boundary glass in nitrogen ceramics by converting it into refractory crystalline phase(s) thus improving the high-temperature properties. Many studies have been carried out to crystallise the grain boundary glass in mixed α–β-sialon ceramics but characterisation of the finished product has always focused on the amount of the residual glass and the type, amount and microstructure of the resulting crystalline oxynitride phase. The present paper is concerned with the effect of heat treatment on the stability and microstructure of both the matrix and grain boundary regions in sialon ceramics.

In this study, densification of sialon ceramics containing selected rare earth oxide additives (Yb_2O_3, Dy_2O_3, Sm_2O_3 either singly or in combination with Y_2O_3) has been studied for pressureless sintered α–β-sialon compositions. Devitrification has been carried out in the range 1000–1450°C using various heat-treatment cycles to eliminate as completely as possible all the grain boundary glassy phase thereby improving high-temperature creep performance. The effect of heat treatment temperature on the α:($\alpha+\beta$)-sialon ratio, microstructure and hence the room temperature mechanical properties has also been investigated.

2 Experimental

Sialon compositions were prepared using powder mixtures of Si_3N_4 (HC Starck-Berlin, Grade LC1), AlN (HC Starck-Berlin, Grade A) and Al_2O_3 (Alcoa, Grade A16SG) as represented by the points 1 and 2 in Fig. 1. A constant molar amount of densifying additive was added to the powder mix, e.g. 6 wt% Y_2O_3, 9·3 wt% Sm_2O_3, 9·9 wt% Dy_2O_3, 10·5 wt% Yb_2O_3 and appropriate intermediate values for mixtures. Sialon compositions of the type to give overall compositions of $(Y,Ln)_{0.053} \cdot Si_{1.77}Al_{0.24}O_{0.35}N_{2.42}$ and $(Y,Ln)_{0.053}Si_{1.71} \cdot Al_{0.32} \cdot O_{0.27}N_{2.47}$ for the points 1 and 2, respectively. Each sample was densified in three ways, using Y_2O_3 to Ln_2O_3 molar ratios 100/0, 50/50, 0/100. Oxygen from added Ln_2O_3 and Y_2O_3 was not taken into account in the calculation of oxygen equivalents.

The starting materials were mixed in water-free isopropanol and milled in rubber-lined mills on a Pascal 12 ball mill for 3 days using sialon milling media. The size of batch used was 50 g. The slurry was then dried and compacts of size 16 × 16 × 6 mm made by die pressing at 125 MPa. Before firing, the specimens were embedded in micron-sized boron nitride powder in graphite crucibles. The sintering was performed in a production furnace of 240 dm^3 volume at 1775°C under nitrogen gas

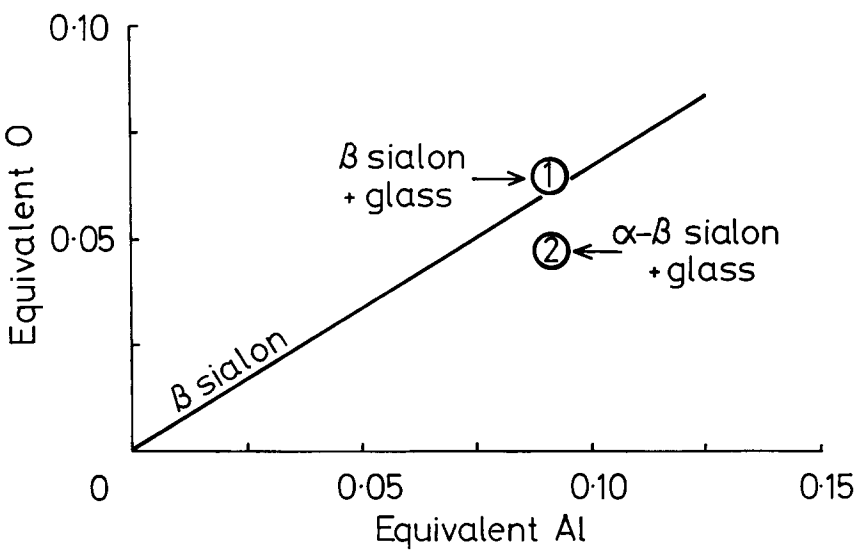

Fig. 1. Overall starting compositions represented as equivalents of oxygen and aluminium added to silicon nitride.

pressure for 2 h. The fully dense, sintered materials were heat treated for 24 h at 1000, 1150, 1300 and 1450 C separately under a nitrogen gas atmosphere in a molybdenum wire-wound alumina tube furnace. Product phases were characterised by X-ray diffraction (XRD) using a Hägg–Guinier camera and CuKα_1 radiation. The computer-linked line scanner (SCANPI LS-20) system, developed by Werner (Arrhenius Laboratory, University of Stockholm, Sweden) was used for direct measurements of X-ray films and refinement of lattice parameters. The amounts of α- and β-sialon phases were found by quantitative estimation from the XRD pattern using the integrated intensities of the (102) and (210) reflections of α-sialon and the (101) and (210) reflections of β-sialon in the following equation:

$$\frac{I_\beta}{I_\alpha + I_\beta} = \frac{1}{1 + K[(1/W_\beta) - 1]} \tag{1}$$

where I_α and I_β are observed intensities of α- and β-sialon lines respectively, W_β is the relative weight fraction of β-sialon, K is the combined proportionality constant resulting from the constants in the two equations, namely

$$I_\beta = K_\beta \times W_\beta \tag{2}$$

$$I_\alpha = K_\alpha \times W_\beta \tag{3}$$

which is 0·518 for $\beta(101)$–$\alpha(102)$ reflections and 0·544 for $\beta(210)$–$\alpha(210)$ reflections.[3] The z-value of the β-sialon phase was obtained from the mean of the z_a and z_c values given by the following equations:

$$z_a = \frac{a - 7{\cdot}6044}{0{\cdot}031} \tag{4}$$

$$z_c = \frac{c - 2{\cdot}9075}{0{\cdot}026} \tag{5}$$

where a and c are calculated unit cell dimensions of β-sialon; JCPDS card 33-1160 was used as a reference for β-Si_3N_4 where $a = 7{\cdot}6044(2)$ Å and $c = 2{\cdot}9075(1)$ Å.

Hardness (HV10) and indentation fracture toughness (K_{IC}) measurements were obtained at room temperature using a Vickers diamond indenter with a 98 N (10 kg) load, and fracture toughness was evaluated according to the method of Evans and Charles.[4]

After application of a carbon coating, polished surfaces of as-sintered and heat-treated samples were examined using a Camscan S4-80 DV scanning electron microscope (SEM) equipped with EDX facilities and a windowless detector suitable for light element analysis.

3 Results and Discussion

3.1 Grain boundary phase characterisation

Pressureless sintering of the more oxygen-rich β-sialon compositions at 1775 C gave fully dense materials for all compositions of dopants. However, when Y_2O_3 was replaced by Yb_2O_3 for the α–β-sialon composition, the product was not dense[5] since the amount of liquid present is less and more nitrogen rich.

Since samples were sintered in a large production furnace at 1775 C, X-ray analysis of the samples after sintering showed additional crystalline grain boundary phase(s). This was attributed to the very slow cooling in the furnace used since the HIPed samples resulted in an entirely glassy grain boundary phase.[6] To obtain consistent results, the sintered samples were therefore re-heated to the sintering temperature, 1775 C, in a small carbon furnace for 15 min and then rapidly cooled to 900 C (2 min total cooling) followed by further cooling to room temperature at $\approx$ 100 C/min to avoid any crystallisation of the oxynitride glass. XRD confirmed this

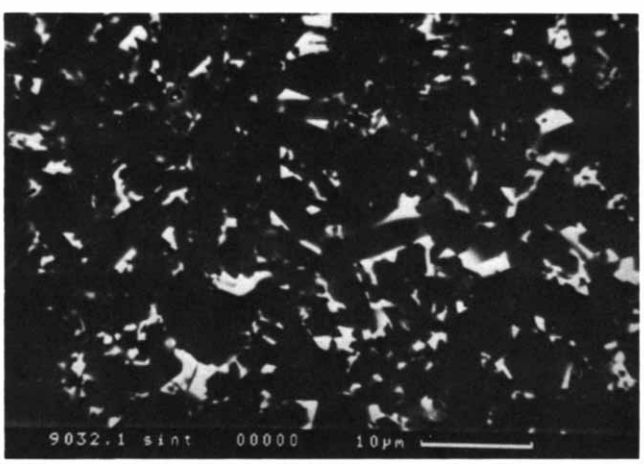

(a)

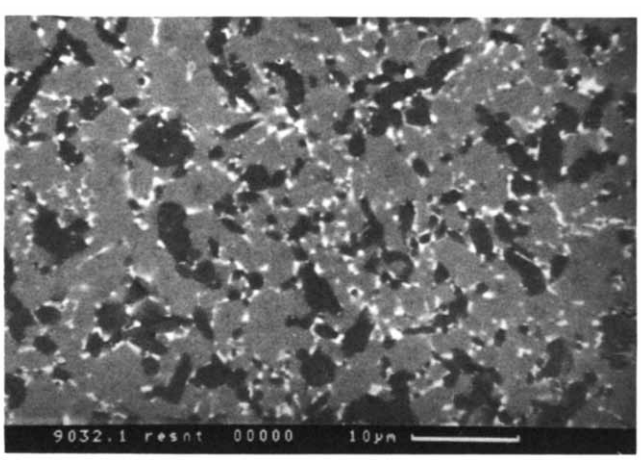

(b)

Fig. 2. Back-scattered SEM micrographs of Yb_2O_3 densified 1775 C pressureless sintered samples: (a) sintered in production furnace, and (b) re-sintered in laboratory furnace and rapidly cooled to room temperature to prevent crystallisation of the grain boundary glass.

but it was noticed that in all samples, the α:β ratio had increased. Thus, the original samples designated β-sialon (point 1 on Fig. 1), now contained some α-sialon, and the original samples designated α–β-sialon (point 2 on Fig. 1) were almost pure α-sialon. The effect was more marked in the case of samples densified with higher atomic number rare earth oxides, e.g. Yb_2O_3. This is clearly apparent also from the microstructures shown in Fig. 2, which correspond to the same sample sintered in the production furnace and re-sintered in the laboratory furnace. Back-scattered electron micrographs very clearly distinguish between the various phases; the β-sialon grains (which contain no rare earth element) are black and more needlelike, whereas the α-sialon grains (which contain a small amount of rare earth element) are grey and more equiaxed whilst Yb-rich crystalline or glassy phases appear fine grained and white, because of the high Yb content. Such a significant change was originally thought to be just a surface phenomenon because of the fast cooling, but Fig. 3 shows that there is no change in the amount or composition of α-sialon at the surface or in the interior of the samples. Originally, it was thought that this effect could be entirely attributed to weight losses occurring during resintering, since $SiO + N_2$ loss would always move the overall composition towards the α-sialon phase region. However, the more detailed heat treatment results described below show that the effect is more marked than can be explained merely by weight loss. The increase in α-sialon content was most marked for high atomic number rare earth additions.

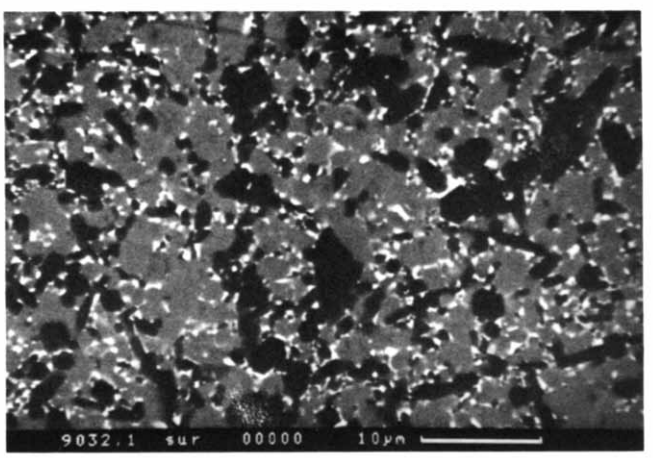

(a)

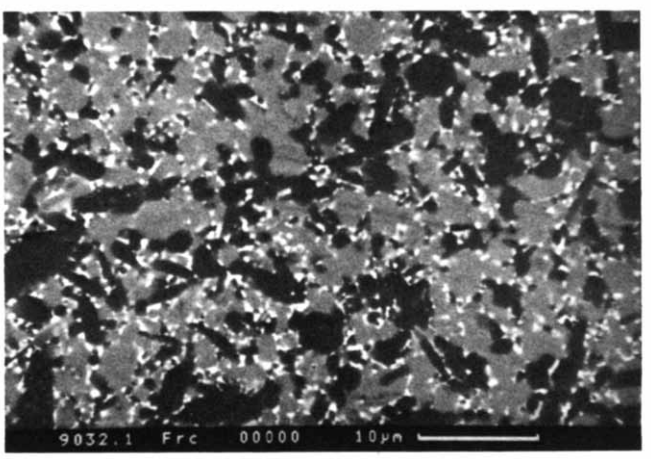

(b)

Fig. 3. SEM micrographs of a fast-cooled Yb_2O_3 densified sample (a) outside surface and (b) polished fracture surface.

X-ray results for subsequent heat treatments of the re-sintered samples performed at temperatures of 1000, 1150, 1300 and 1450°C and the resulting phase assemblages are given in Fig. 4. Several combinations of crystalline secondary phases occur and these are consistent with previous heat treatment data reported for these compositions sintered by HIP.[7]

In β-sialon starting compositions, B-phase (Ln_2SiAlO_5N) easily devitrified at 1000°C from grain boundary glasses prepared from low-atomic-number rare earths, whereas J phase ($Y_4Si_2O_7N_2$) occurred in Yb- and mixed Y–Yb-doped systems. Two different compositions of B-phase were observed for rare earth elements between Yb and Sm (see Fig. 5). The reason for these two compositions is not well understood but it is thought that the first composition was produced during cooling from the sintering temperature and the second one was produced during heat treatment. In Sm–Si–Al–O–N compositions, the ionic radius of Sm is too large to devitrify B-phase and therefore the combination of U-phase ($Sm_3Si_3Al_3O_{12}N_2$) plus wollastonite ($SmSiO_2N$) is produced instead.

B-phase was replaced by a garnet phase when the heat treatment temperature was increased to 1050–1150°C. J phase was observed with garnet up to 1400°C in Yb and Y–Yb systems and wollastonite formed in all other systems except Sm. Because of ionic size, a garnet phase is not stable in the Sm system, and U plus samarium aluminate ($SmAlO_3$) remains the stable phase assemblage up to 1400°C.

For α–β-sialon starting compositions, Fig. 4(b) shows that the stability regions for B and garnet remain the same as for β-sialon compositions but no other crystalline phases (e.g. J-phase or wollastonite) were observed. This is because of the more Ln- and N-rich starting composition. The products are also more α-sialon rich than the β-sialon materials and since α-sialons can accommodate all available elements into the structure, there is less residual glass but this still crystallises as either B or a garnet phase, similar to the β-sialon compositions. Because of the large size of Sm^{3+}, samarium aluminate is again the major phase observed in Y–Sm and Sm-densified sialons (instead of garnet) and in addition to this phase, an aluminium containing melilite phase was observed at 1400°C. In 1000–1100°C heat-treated

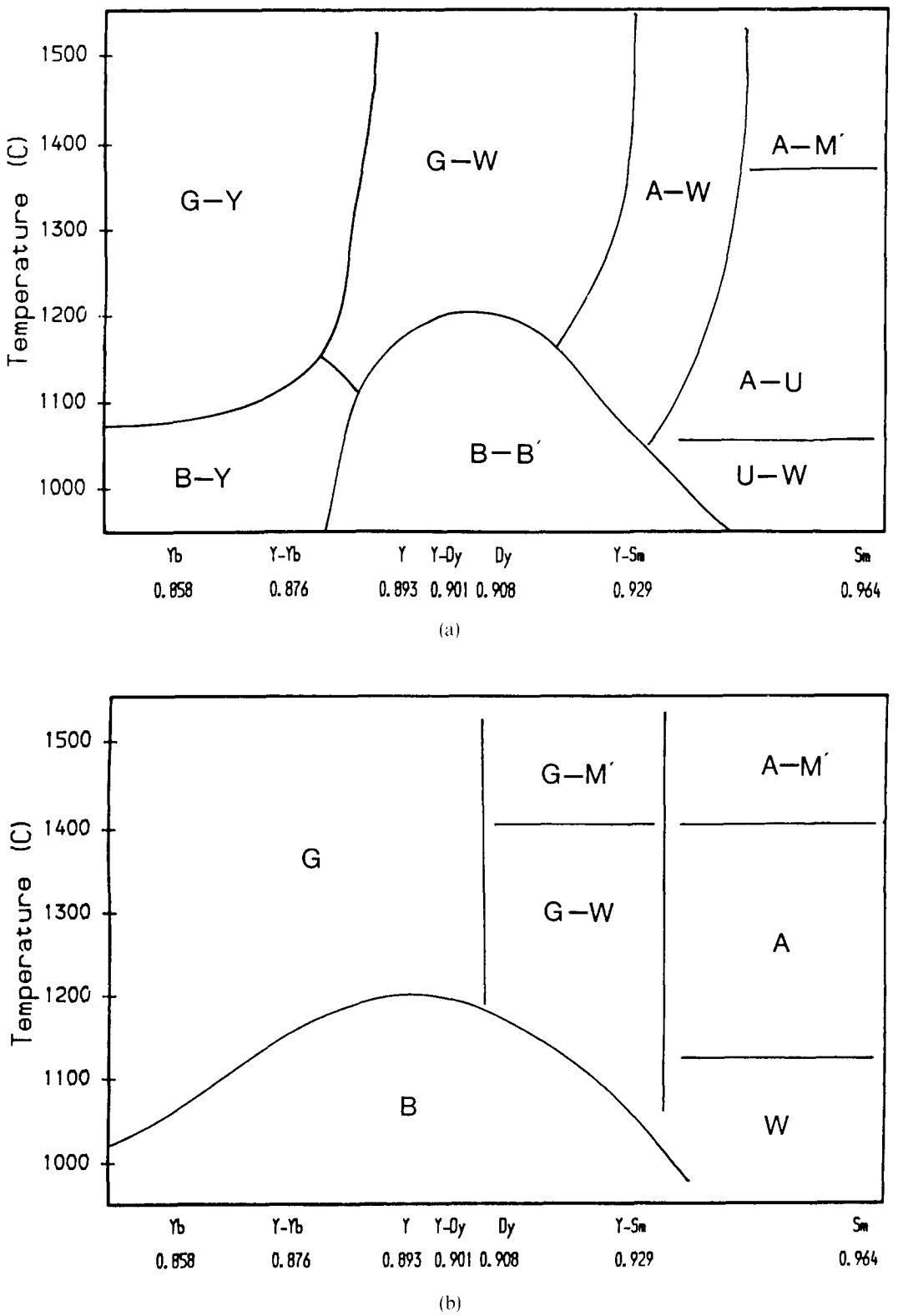

Fig. 4. Heat treatment of 1775°C pressureless sintered (a) β-sialon, and (b) α–β-sialon materials. B, B-phase [$(Y, Ln)_2SiAlO_5N$]; W, wollastonite [$(Y,Ln)SiO_2N$]; U, U-phase [$Ln_3Si_3Al_3O_{12}N_2$]; Y, J-phase [$(Y, Ln)_4Si_2O_7N_2$]; G, garnet [$(Y, Ln)_3Al_5O_{12}$]; A, aluminate [$LnAlO_3$]; and M′, melilite [$Ln_2Si_3O_3N_4$], with some substitution of Si and N by Al and O.

Sm-containing compositions, wollastonite is the only crystalline oxynitride observed instead of B-phase.

Back scattered SEM micrographs of 1775°C pressureless sintered samples are shown in Fig. 6 after further heat treatment. As with the sintered samples several differences in microstructure were observed on moving to lower Z rare earths, namely

(a) the β-sialon grains became more needlelike,
(b) the α-sialon content decreased, and
(c) the amount of intergranular phase increased.

These differences were observed in β-sialon starting compositions but they were significantly more marked for the α–β-sialon compositions.

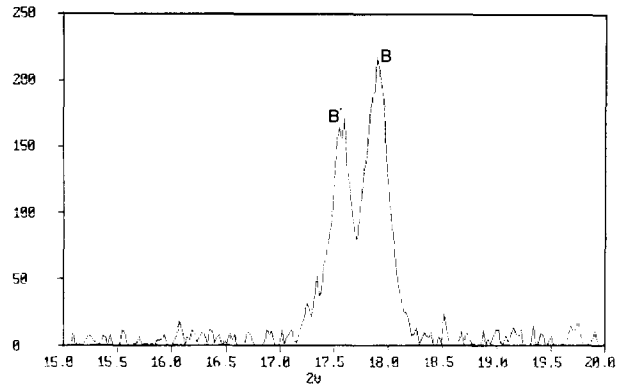

Fig. 5. Part of the X-ray pattern of Dy-densified β-sialon material heat treated at 1150°C, showing two different B-phase compositions.

3.2 $\alpha \rightleftharpoons \beta$-sialon transformation

In addition to the differences already discussed in the type of secondary crystalline phase(s) formed in the different rare earth systems, the other noticeable difference in behaviour was the change in $\alpha:(\alpha+\beta)$-sialon ratio on heat-treating at different temperatures. In this case $\alpha \rightarrow \beta$ reaction occurred and the $\alpha:(\alpha+\beta)$-sialon ratio in all samples dramatically decreased. This was again most marked for the higher atomic number rare earth oxide sintering additives. Thus, for example, the Yb_2O_3-densified sample, shown in Fig. 2, which, after initial pressureless sintering at 1775°C was identified as containing 10% α-sialon and 90% β-sialon, and after re-sintering for 15 min at 1775°C changed to 80% α-sialon and 20% β-sialon, dramatically changed to 10% α–90% β after 1450°C heat treatment, 30% α–70% β after 1300°C heat treatment, 50% α–50% β after 1150°C heat treatment, and 70% α–30% β after 1000°C heat treatment. Similar transformation was also observed for other sintering additives and the resulting $\alpha:(\alpha+\beta)$ ratios are shown in Fig. 7. Spacie[8] and Cheng[9] also observed similar transformations during heat treatment of Y- and Sm-sialons, respectively, but they did not give any explanation. The microstructures of these samples also clearly confirm the changes in $\alpha:(\alpha+\beta)$ ratio that occur, Fig. 8 showing the effect for Yb_2O_3-densified

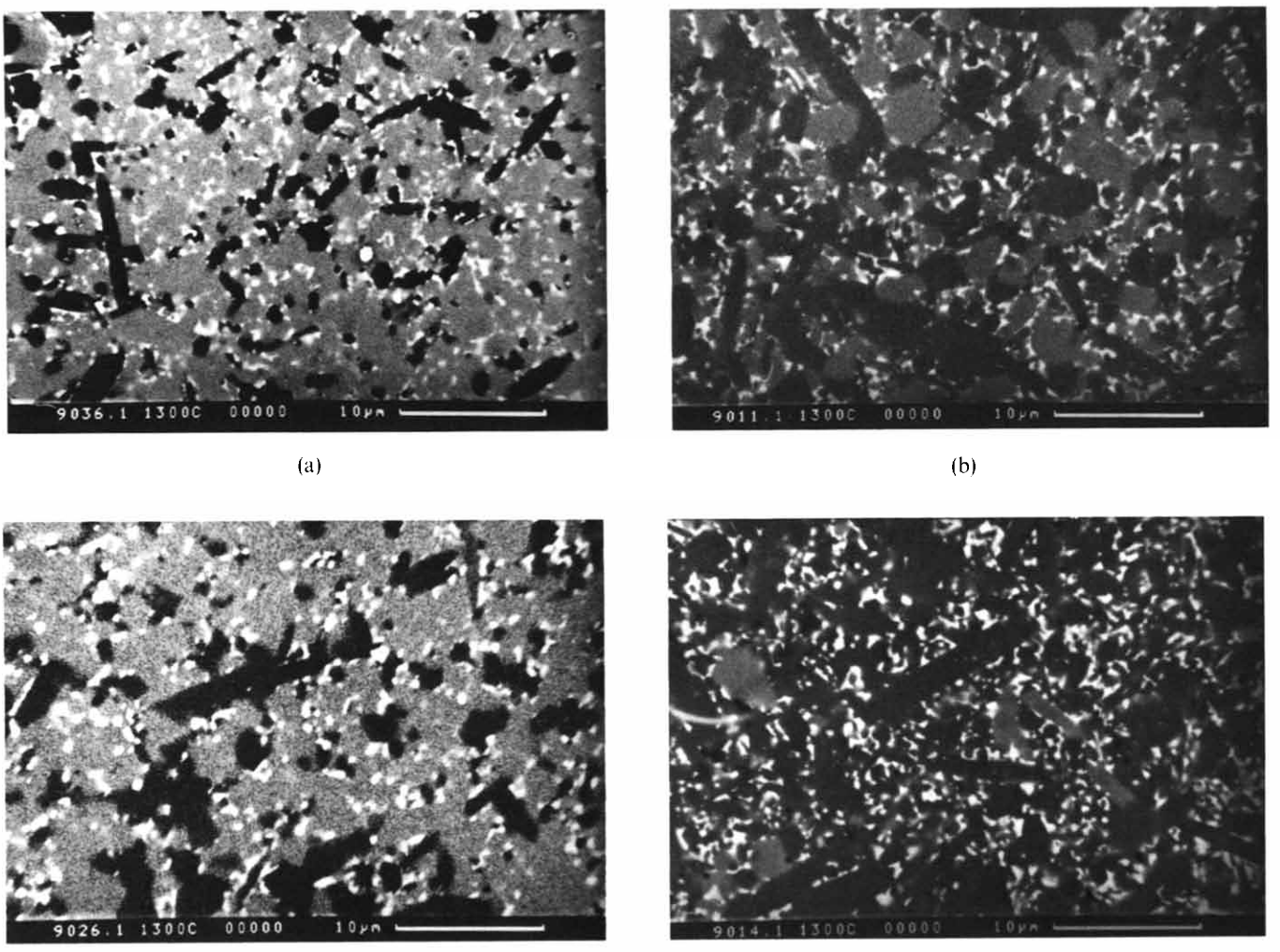

Fig. 6. SEM micrographs (back-scattered mode) of 1775°C pressureless sintered α–β-sialon compositions after heat treatment at 1300°C. The sintering additives used were (a) Yb_2O_3, (b) Y_2O_3, (c) Dy_2O_3 and (d) Sm_2O_3.

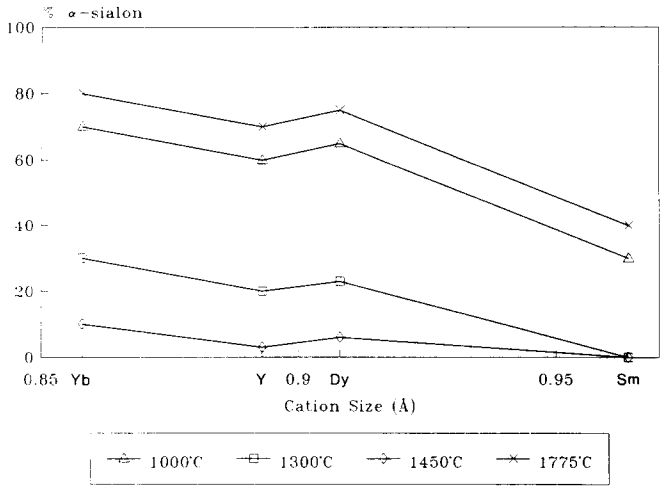

Fig. 7. $\alpha:(\alpha+\beta)$ ratio in α-β sialon samples densified with different sintering additives and different heat-treatment temperatures.

materials. Clearly, systematic differences occur on increasing the heat treatment temperature, namely

(a) the β-sialon grains become more needlelike,
(b) the α-sialon content decreases, and
(c) the amount of intergranular phase increases.

These changes in microstructure are associated with a reduction in β-sialon z-value from 0·84 to 0·63 (see Fig. 9) and also with a slight decrease in α-sialon unit cell dimensions (e.g. for Yb, a and c change from 7·8055 and 5·6926 Å at 1000 °C to 7·7952 and 5·6822 Å at 1450 °C, respectively) as the heat-treatment temperature increases. These changes can be correlated with removal of Al and O from both the matrix and grain boundary glass as the YbAG phase starts to form at 1250 °C. Taking the now mainly β-sialon product above 1580 °C once again causes the reverse (i.e. $\beta \rightarrow \alpha$) transformation to occur (Fig. 10), with reformation of the original large α-sialon grains.

Another interesting feature of the microstructures is the change in α-sialon grain size. In the initial 1775 °C sintered sample, the grain size is quite large (typically 2–3 μm) and this is substantially preserved at 1000 °C, because this temperature is too low for much change to occur even though the higher heat treatment temperature results show that α-sialon is probably unstable with respect to β-sialon, but the kinetics are too slow for transformation to occur. At 1150 °C, some $\alpha \rightarrow \beta$-sialon transformation has occurred, and each α-sialon grain has split up into smaller grains of β-sialon plus additional grain

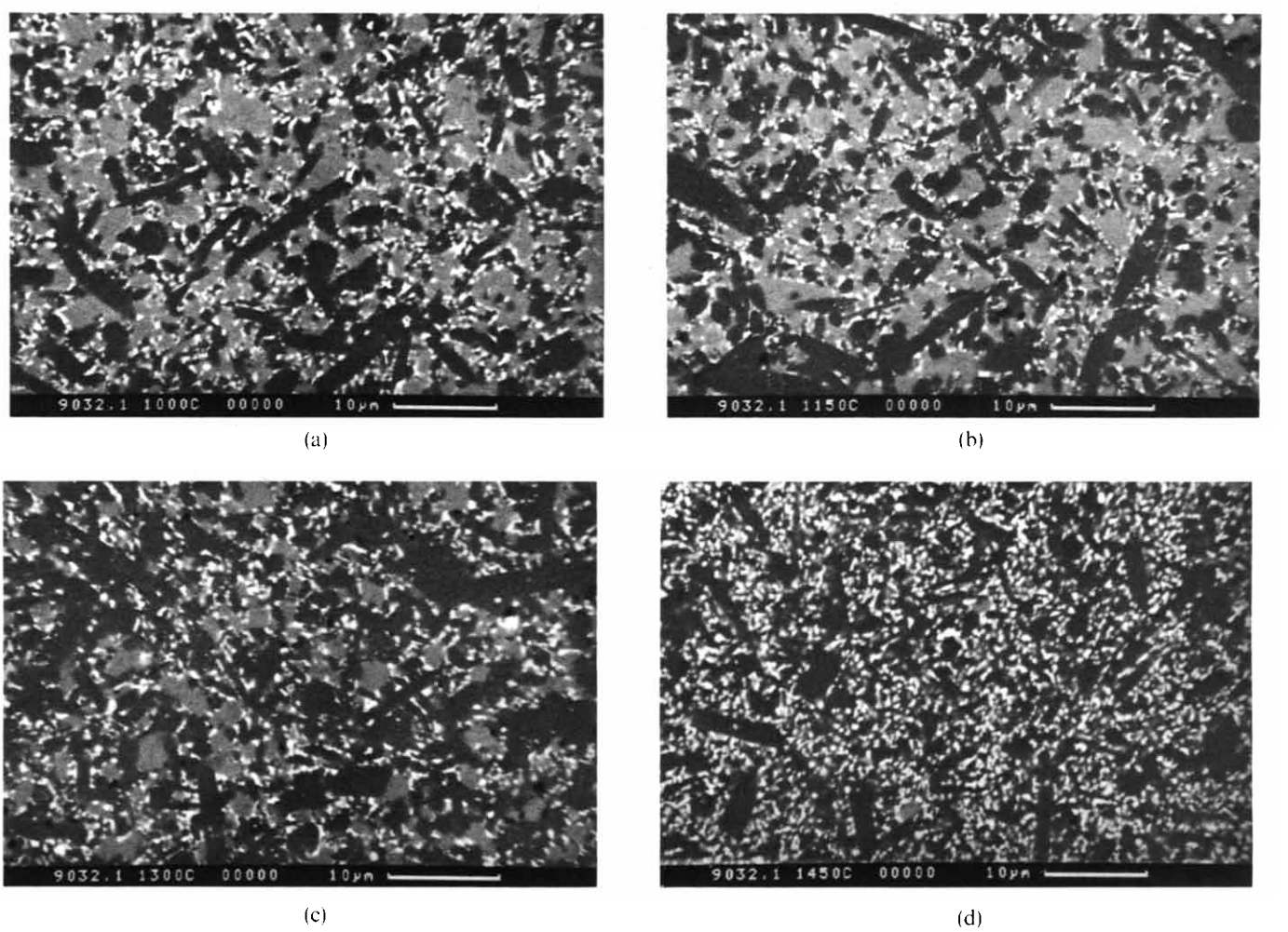

Fig. 8. SEM micrographs of the Yb_2O_3 densified sample shown in Fig. 2 after further heat treatment at (a) 1000 °C, (b) 1150 °C, (c) 1300 °C, and (d) 1450 °C.

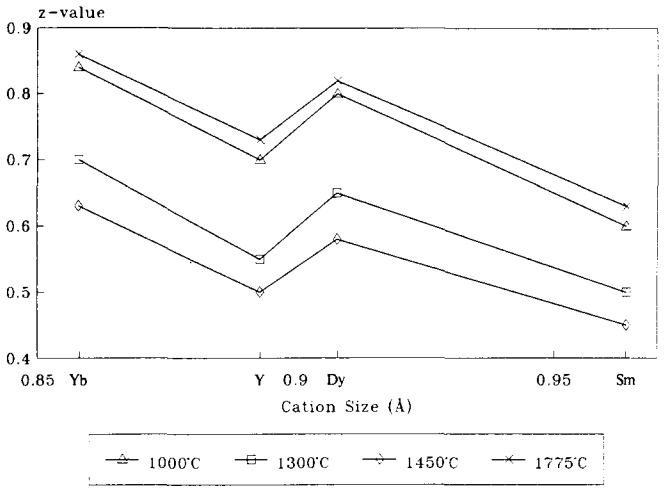

Fig. 9. z-Values of the β-sialon phase in mixed α–β-sialon samples after further heat treatment as a function of sintering additive and heat treatment temperature.

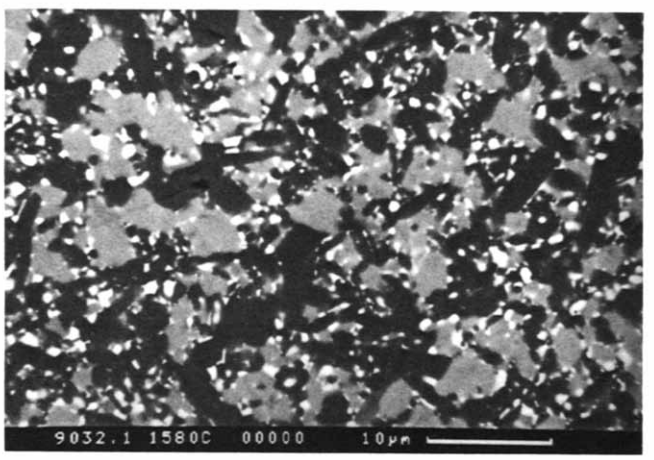

Fig. 10. SEM micrograph of Yb_2O_3 densified sample shown in Fig. 8 after 1580 C heat treatment.

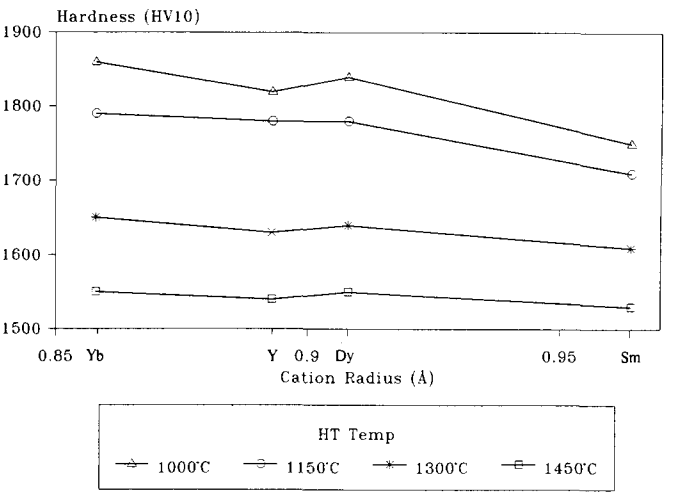

Fig. 11. The Vickers hardness (HV10) of pressureless sintered β-sialon ceramics as a function of ionic size of rare earth cation and heat-treatment temperature.

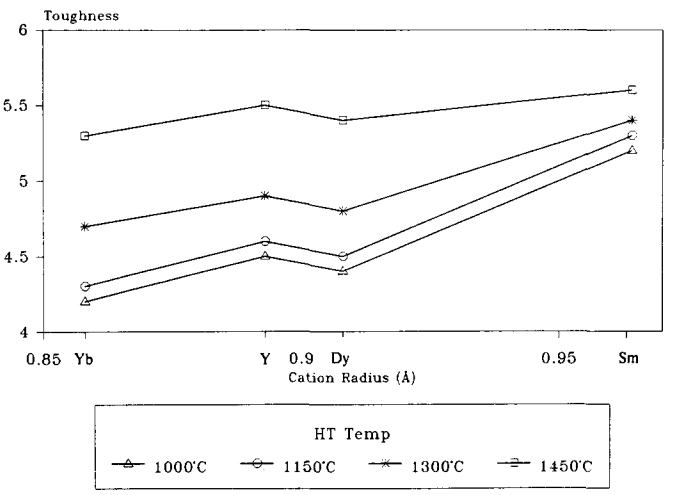

Fig. 12. The fracture toughness of pressureless sintered β-sialon ceramics as a function of ionic size of rare earth cation and heat-treatment temperature.

boundary material. This process becomes more marked at the higher heat treatment temperatures, so that the microstructures of the 1450°C heat treated samples consist of large (up to 10 μm in length) β-sialon needles surrounded by a finer matrix of α-sialon plus other grain boundary phase(s).

The above figures show that the trends in % α-sialon and z-value of the β-sialon phase strongly correlate with each other. This relationship also has a bearing on mechanical properties and provides a useful guide to the high temperature properties of sintered and heat treated materials. This is because the β-sialon z-value correlates with the aspect ratio of the β-sialon grains, with Yb having the highest z-value (equiaxed grains) and Sm the lowest z-value (needle-shaped grains). The ionic size of the sintering additive is the major factor influencing the α–β-sialon ratio just as in the case of pressureless sintered β-sialons.

The results of hardness (HV10) and indentation fracture toughness (K_{IC}) measurements are presented in Figs 11 and 12 as a function of heat treatment temperature. Although there have not been many publications on the hardness of mixed α–β-sialons, it is generally accepted that the hardness increases with the amount of α-sialon present. Because hardness is determined by the Burgers vector associated with dislocation movement through the lattice, and the c axis of α-sialon ($c_{\alpha'} = 5{\cdot}62$ Å) is more similar to the a-axis ($\alpha_{\beta'} = a_{\alpha'} = 7{\cdot}60$ Å) than is the c-axis of β-sialon ($c_{\beta'} = 2{\cdot}91$ Å), [001] type dislocations in this direction are favoured whereas in α-sialon, the larger Burgers vector corresponds to a higher resistance to dislocation motion in the c-axis and hence a higher hardness. Another reason for the increase in hardness is the smaller amount of intergranular phase in α-sialon compositions since the α-phase can accommodate the metal cation from the sintering additive. Since the amount of α-sialon changes with devitrification temperature, the hardness also shows similar trends, decreasing with increasing temperature.

Since the fracture toughness of sialon ceramics

can be correlated with grain shape, single phase, high aspect ratio β-sialon microstructures are significantly tougher than the more equiaxed α-sialon microstructures and more easily permit crack deflection as a mechanism for toughening.[10] Since the current observations show that α-sialon grains split into smaller, more elongated grains of β-sialon + grain boundary phase during heat treatment, this provides more complex possibilities for crack deflection. As a result, toughness is increased as the heat treatment temperature is increased up to 1550°C in direct proportion to the extent of $\alpha \rightarrow \beta$ transformation.

4 Conclusions

Microstructural and mechanical property characterisation of α–β-sialon ceramics show that especially for high atomic number rare earth oxide densified materials, the α-sialon phase is only stable at high temperatures (typically $\approx$ 1550°C) and transforms to β-sialon plus other Ln-rich grain boundary phases at lower temperatures. This reversible reaction can be easily controlled by time and heat-treatment temperature and offers an excellent mechanism for controlling the mechanical properties of the final material. The range of α:($\alpha + \beta$) ratios observed over the complete range of heat-treatment temperatures used (1000–1800°C) is more than can be explained by the α-sialon phase region changing in size with temperature. If indeed the results are taken at face value, they indicate more about the restrictive nature of the α-sialon interstices with respect to the size of the cation being inserted. Thus, for example, La and Ce are too big to go into α-sialon, and Yb, even though stabilising α-sialon better than the rest at 1800°C is too small to stabilise an α-sialon structure below $\approx$ 1600°C.

References

1. Jack, K. H., Sialon hardmetal materials. In *Proc. 2nd Int. Conf. Science Hard Mater.*, ed. E. A. Almond, C. A. Brookes & R. Warren. Adam Hilger Ltd, Bristol, UK, 1986, pp. 363–76.
2. Ekström, T. & Ingelström, I., Characterization and properties of sialon materials. In *Proc. Int. Conf. Non-oxide Technical and Engineering Ceramics*, ed. S. Hampshire. Elsevier Applied Science, London, UK, 1986, pp. 231–53.
3. Liddell, K., X-ray analysis of nitrogen ceramic phases. MSc thesis, University of Newcastle upon Tyne, UK, 1979.
4. Evans, A. G. & Charles, A., Fracture toughness determination by indentation. *J. Am. Ceram. Soc.*, **59** (1976) 371–2.
5. Liddell, K., Mandal, H., Thompson, D. P. & Ekström, T., Sialon ceramics sintered with additions of Yb_2O_3, Dy_2O_3 and Sm_2O_3 or as mixtures with Y_2O_3 (to be published).
6. Mandal, H., Thompson, D. P. & Ekström, T., Heat treatment of sialon ceramics densified with higher atomic number rare earth and mixed yttrium rare earth oxides. In *Proc. Special Ceramics 9*. The Institute of Ceramics, Stoke-on-Trent, UK, 1992, pp. 97–104.
7. Mandal, H., Thompson, D. P. & Ekström, T., Heat treatment of Ln–Si–Al–O–N glasses. In *Proc. 7th Irish Mater. Forum Conf. IMF7*, ed. M. Buggy & S. Hampshire. Trans. Tech Publications, Switzerland, 1992, pp. 187–203.
8. Spacie, C. J., Characterization and heat treatment of sialon ceramics. PhD thesis, University of Newcastle upon Tyne, UK, 1984.
9. Cheng, Y., Internal Report, University of Newcastle upon Tyne, UK, 1991.
10. Lewis, M. H., Leng-Ward, G. & Jasper, C., Sintering additive chemistry in controlling microstructure and properties of nitride ceramics. In *Ceramic Translations I*, ed. G. L. Messing, E. R. Fuller and H. Hausner, Am. Ceram. Soc. Inc., Westerville, Ohio, USA, 1988, pp. 1019–33.